

Studies of Low-Mass Star Formation with ALMA

Neal J. Evans II

*Department of Astronomy, The University of Texas at Austin Austin,
TX 78712-1083*

Abstract. ALMA will revolutionize the study of star formation by providing a combination of angular resolution and sensitivity that far exceeds that of present instruments. I will focus on studies of relatively isolated cores that are forming low-mass stars. There is a general paradigm for the formation of such stars, and there are detailed theoretical predictions for the evolution of the density and velocity fields for different assumptions about the initial conditions. Because the theory is well developed, observational tests are particularly revealing. The primary probes of physical conditions in these regions are discussed and the sensitivity of ALMA to these probes is shown and compared to the current state of the art. The consequences for the ALMA requirements are discussed.

1. Introduction

The focus in this paper will be on regions forming low mass stars in relative isolation, as other papers are covering issues of massive star formation and clustered star formation. Isolated star formation is interesting for several reasons. An empirical evolutionary scheme (Lada 1987, André et al. 1993) is generally accepted. There is a well-established theory (Shu et al. 1987) and variations (e.g., Foster & Chevalier 1993; Henriksen, André, & Bontemps 1997; McLaughlin & Pudritz 1997) that can be tested by observations. It is particularly suited to studies connecting star formation to planet formation.

The two primary probes of the conditions in star-forming cores are continuum emission from dust and spectral lines from molecules. These are complementary in many ways. The dust emission is not affected by molecular depletion and traces column density very effectively, but dust grain sizes may be a function of the environment, or gas and dust distributions may differ because of ambipolar diffusion. In principle, molecular spectroscopy probes the local density and velocity fields, but it is sensitive to variations in chemical abundances. Together, these two probes can be very powerful. With ALMA, a hybrid probe will become widely available: molecular line absorption against emission from compact dust components, such as circumstellar disks.

The exquisite sensitivity of ALMA to continuum emission will allow us to map the detailed structure of the dust column density in many cores, ranging along the evolutionary sequence, to trace the flow of matter from large scales to disks and stars. Together with information from other wavelength regions, a

complete picture of the distribution of dust temperature and column density will result, along with information on possible changes in the grain size distribution.

Maps of optically thin, thermally excited tracers will provide column densities of gas, for comparison to those of dust measured by the continuum emission. The molecular spectroscopy of lines with subthermal excitation will yield direct estimates of the local density. Combined studies of optically thick and thin lines will reveal the kinematics in detail. Finally, absorption spectroscopy of the material in front of opaque disks will be a new capability of ALMA that will help to unravel the complex velocity fields involved in forming stars.

The dust continuum emission provides a probe of mass (M), total gas column density (N), dust temperature (T_D), grain properties, and the component of the magnetic field projected on the sky (B_\perp). Molecular line emission can probe the gas kinetic temperature (T_K), volume density (n), velocity field (v), abundances (X), and the line-of-sight component of the magnetic field (B_\parallel). A more detailed discussion of these probes can be found in Evans (1999).

2. Dust Continuum Emission

The dust continuum emission provides a probe of the total amount and distribution of the dust. If the dust and gas are well mixed, these quantities can be translated into the same information about the gas. One caveat is that the dust opacity may change from source to source or even within a single source (e.g., Visser et al. 1998). The primary tool that has been used in the past is the spectral energy distribution, or SED ($S_\nu(\lambda)$), which gives information on the source luminosity, by integrating under the SED. The mass can be determined by observing the flux in large beams at λ large enough that the emission is optically thin. With suitable radiative transport codes (e.g. Egan, Leung, & Spagna 1988), source models constrained by the SED can yield the distribution of the dust temperature ($T_D(r)$) for a given set of grain properties. Matching different parts of the SED can constrain the choice of grain opacities (Adams, Lada, & Shu 1987; Butner et al. 1991; van der Tak et al. 1999).

More recently, spatially resolved studies of the intensity of dust continuum emission have become a powerful probe. New instruments operating at submillimeter wavelengths have provided an enormous increase in this kind of data (e.g., Johnstone & Bally 1999; Motte, André, & Neri 1998). Maps of polarized dust emission are starting to provide maps of B_\perp (Greaves et al. 1999; Rao et al. 1998). By taking cuts through maps or by azimuthally averaging the intensity, one obtains $I(b)$, the intensity as a function of impact parameter (b), the separation of the beam from the center of emission. Plots of $I(b)$ provide probes of column density as a function of impact parameter $N(b)$, and with modeling, the density distribution $n(r)$, which is predicted by theories of isolated low-mass star formation. Recent examples of such studies are those of Chandler & Richer (2000), Hogerheijde & Sandell (2000) and Shirley et al. (2000). They reveal steeper density gradients than were apparent from most studies of molecular lines. An example of an SED and determinations of $I(b)$ are shown in Fig. 1 for B335, a well-studied region of low mass star formation.

Interferometers naturally provide a complementary probe to $I(b)$, the spatial visibility function ($S(uvdist)$), which can also be compared to models. This

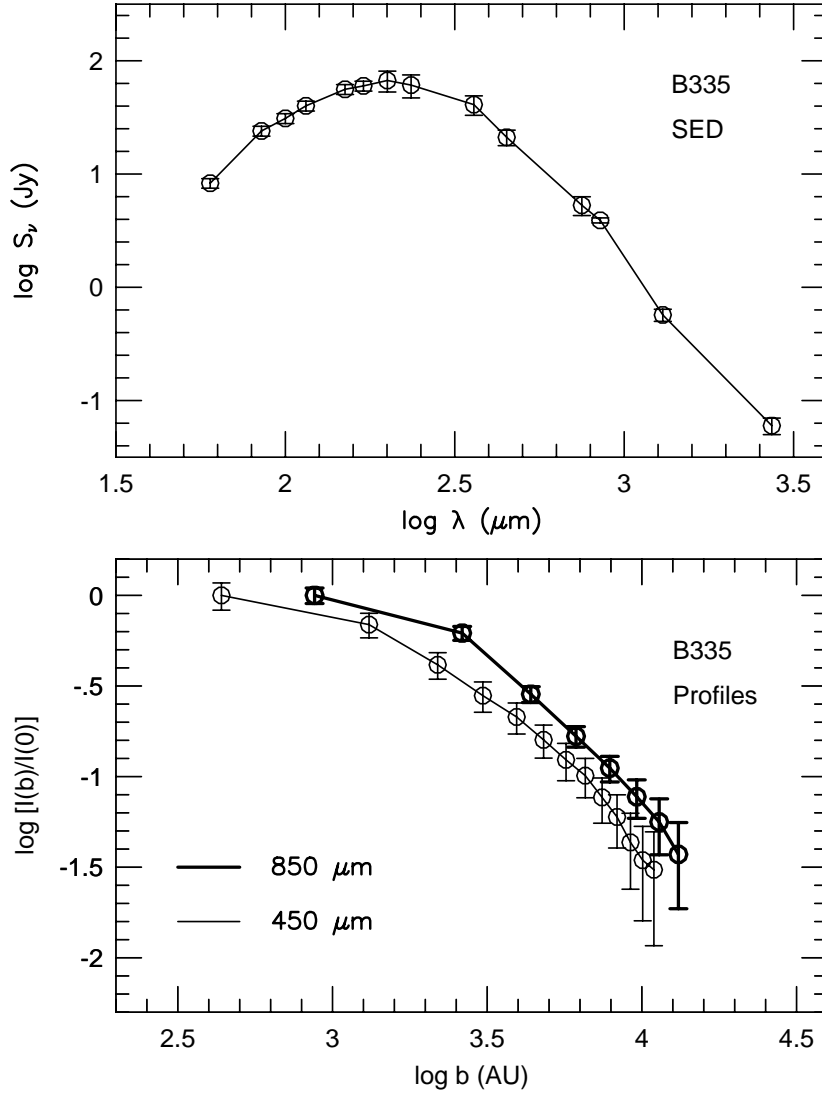


Figure 1. The top panel is the SED for B335, an isolated core at a distance of 250 pc, which is forming a low-mass star. References to the photometry can be found in Shirley et al. (2000). The bottom panel shows the normalized radial intensity profiles from SCUBA maps at 850 and 450 μm versus the impact parameter in AU (Shirley et al. 2000).

approach is especially well suited to distinguishing compact structures, such as disks, from the envelope. An example of how this capability can separate components that would be otherwise indistinguishable is given in Fig. 2, taken from Looney, Mundy, & Welch (1997).

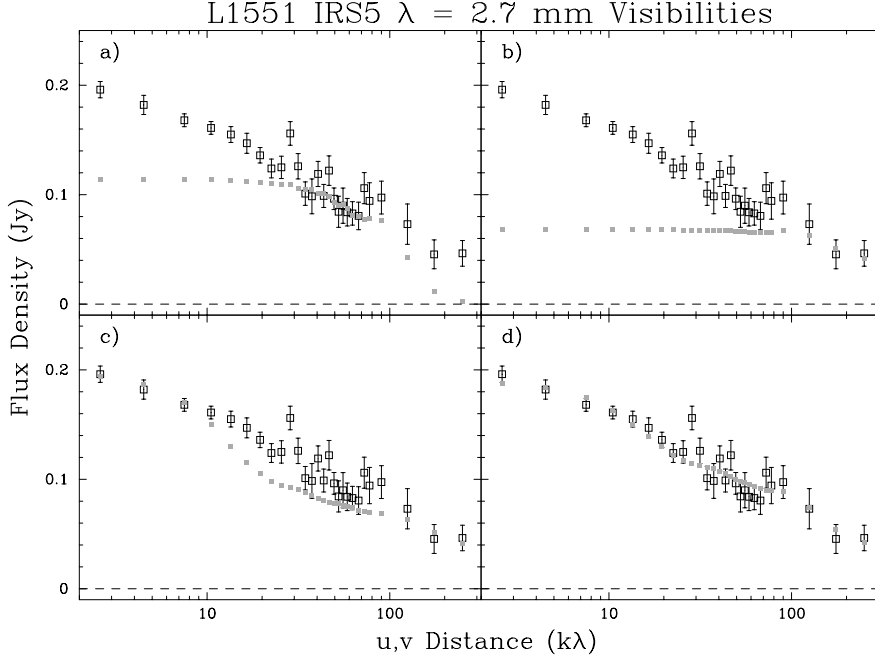


Figure 2. Observed visibilities of L1551 IRS 5 at 2.7 mm, binned in annuli (open squares with error bars), are plotted versus the projected baseline in units of 10^3 times the wavelength. Different models are shown in each panel by the small boxes. Panel a has a model with only a Gaussian source of radius 80 AU; panel b has a model with two point sources constrained to match the map; panel c adds a truncated power law envelope to the two point sources; panel d adds to the previous components a circumbinary structure, represented by a Gaussian. In the final optimization (panel d), the envelope has a mass of $0.28 M_{\odot}$ and an outer radius of 1100 AU, the circumbinary structure has a mass of $0.04 M_{\odot}$, and the circumstellar disk masses are 0.024 and $0.009 M_{\odot}$ (Looney et al 1997).

To discuss the sensitivity of ALMA to dust continuum emission, we make some simplifying assumptions: the Rayleigh-Jeans limit is valid; the emission is optically thin; the dust opacity follows

$$\kappa_{\nu} = 9.0 \times 10^{-26} \text{cm}^2 \text{H}_2^{-1} \lambda_{\text{mm}}^{-1}; \quad (1)$$

and the resolution is diffraction-limited ($\theta_b = 1.2\lambda/B$, where B is the maximum dimension of the array). Then the sensitivity to dust emission can be expressed in terms of the product of gas column density and dust temperature:

$$NT_D = 2.5 \times 10^{24} \lambda_{\text{mm}} B_{\text{km}}^2 \Delta S_\nu (\text{mJy}) \quad (2)$$

or, in terms of visual extinction,

$$A_V T_D = 2.5 \times 10^3 \lambda_{\text{mm}} B_{\text{km}}^2 \Delta S_\nu (\text{mJy}). \quad (3)$$

Alternatively, one can describe the sensitivity to gas mass in Earth masses given a distance (d):

$$MT_D = 470 M_\oplus (d/140 \text{ pc})^2 \lambda_{\text{mm}}^3 \Delta S_\nu (\text{mJy}). \quad (4)$$

The fiducial distance of 140 pc is a typical distance to nearby regions that are forming low-mass stars. These equations can be generalized to the case where the Rayleigh-Jeans approximation fails, at the cost of some clarity. These expressions will suffice to illustrate the main points, if we bear in mind that Rayleigh-Jeans failure will first tend to decrease the sensitivity to column density or mass at the shorter wavelengths.

In calculating sensitivities, I have used the values of $\Delta S_\nu (\text{mJy})$ given by Butler & Wootten (1999), for 1.5 mm of precipitable water vapor (PWV). The values are for 1σ noise after 60 sec of integration. This would correspond to 22σ in an 8 hour integration. The resulting plots of NT_D and MT_D versus λ are shown in Fig. 3, along with a plot of the spatial resolution in AU at a distance of 140 pc. The plot is truncated at 3 mm to allow the shorter wavelengths to be seen clearly. Note that $\lambda \geq 1$ mm have comparable sensitivity to column density, with much better sensitivity in compact configurations. For the most compact configuration, ALMA could detect $5.5 \times 10^{20} \text{ cm}^{-2}$ ($A_V = 0.55 \text{ mag}$) at $T_D = 10 \text{ K}$. The sensitivity to mass is best at $\lambda = 0.87 \text{ mm}$ for the standard water vapor. The mass sensitivity is even better at the shortest wavelengths if the PWV drops to 0.35 mm (crosses in the top panel), but only if the dust is warm enough that the Rayleigh-Jeans limit applies ($T_D \gg 41 \text{ K}$ at 850 GHz).

To put things in perspective, ALMA can detect the dust emission from $0.3 M_\oplus$ of gas at $T_D = 100 \text{ K}$ at $\lambda = 0.87 \text{ mm}$! Another useful comparison is to the current state of the art. Table 1 shows the comparison between ALMA and SCUBA on the JCMT, assuming roughly comparable PWV, at $\lambda = 0.87 \text{ mm}$.

Table 1. ALMA versus SCUBA for Dust Continuum Emission

Quantity	SCUBA	ALMA	
		$B = 0.2 \text{ km}$	$B = 10 \text{ km}$
$\Delta S_\nu (\text{mJy})$	40	0.11	0.11
$\theta_b (\text{arcsec})$	15	1.1	0.02
$\theta_b (\text{AU at } 140 \text{ pc})$	2100	150	3.0
$A_V T_D (\text{mag-K})$	19	9.6	2.4×10^4
$M_\oplus T_D (\text{at } 140 \text{ pc})$	1.2×10^4	34	34

It is clear from the figure and table that ALMA will take us into new regimes of sensitivity and resolution, allowing study of $N(b)$ and hence $n(r)$ to

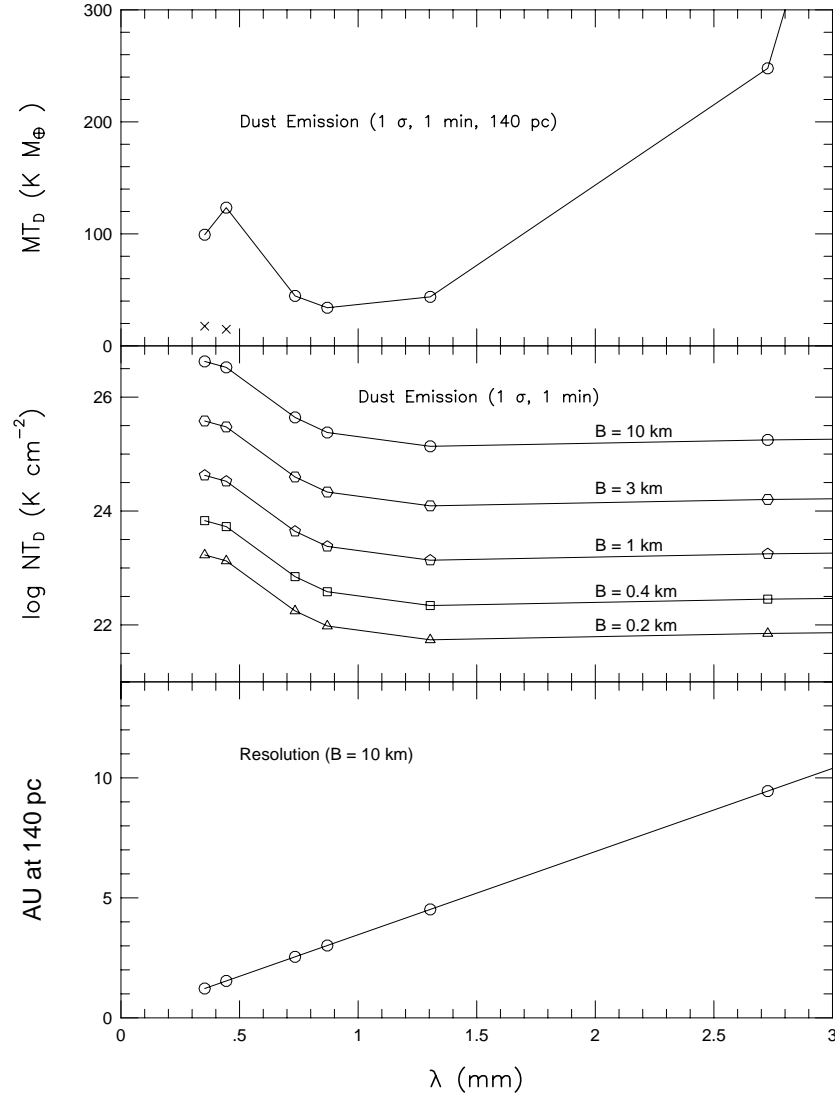


Figure 3. Sensitivity to mass (top) versus wavelength for a distance of 140 pc. The crosses at the bottom left correspond to PWV of 0.35 mm; all other points are for 1.5 mm. Sensitivity to column density (middle) versus wavelength, for a maximum baseline of 10, 3, 1, 0.4 and 0.2 km. Note the logarithmic scale on this panel. Bottom plot shows resolution in AU at 140 pc, the distance of many star forming regions, for a maximum baseline of 10 km.

much finer scales than currently possible. The key requirement for this work is spatial dynamic range. Sensitivity to the largest relevant spatial scales is a challenge for any interferometer, and ALMA must solve this problem.

3. Molecular Line Emission

Mapping molecular line emission provides a wealth of information about star forming regions. Transitions between levels in thermal equilibrium (CO, some transitions of H_2CO , CH_3CN , etc.) provide T_K , while transitions between levels not in thermal equilibrium allow a measure of n . The latter however is coupled to the abundance because of trapping, and multiple transitions of a single molecule are needed to separate these effects. In the simplest model, a homogeneous cloud, one derives a weighted mean density along each line of sight. For more sophisticated models (e.g., power laws and collapse models), the data constrain the model parameters.

The line profiles contain vital information about the velocity field. While this has been difficult to extract, in some cases it is possible to learn about rotation (Goodman et al. 1993), infall (Myers, Evans, & Ohashi 2000), and outflow (Bachiller 1996). For a few transitions, the line profile, observed with suitable polarization, yields B_{\parallel} (e.g., Crutcher 1999).

The key instrumental parameters for molecular line emission are the beam size and the velocity resolution. Butler & Wootten (1999) give the formula for the line radiation temperature (proportional to intensity) for the case of diffraction-limited beams and velocity resolution of 1 km s^{-1} :

$$\Delta T_R = 0.32 \text{ K } B_{\text{km}}^2 \Delta S_1 (\text{mJy}). \quad (5)$$

While bright lines may be observed with diffraction-limited beams, choosing a fixed beam of $1''$ provides a convenient benchmark for weak lines. In this case,

$$\Delta T_R = 0.013 \text{ K } \frac{\lambda_{\text{mm}}^2 \Delta S_1 (\text{mJy})}{(\theta_b/1'')^2 \sqrt{\delta v} (\text{km s}^{-1})} \quad (6)$$

where $\Delta S_1 (\text{mJy})$ is the sensitivity (1σ in 60 sec) in a 1 km s^{-1} band from Butler & Wootten (1999), and $\delta v (\text{km s}^{-1})$ is the velocity resolution in km s^{-1} .

The current state of the art for interferometers using $\theta_b = 1''$ is about 1000 mJy at 110 GHz. For ALMA, $\Delta S_1 (\text{mJy})$ is less than 10 mJy up to 345 GHz, implying a gain of a factor of 100. Values of $\Delta T_R < 0.5 \text{ K}$ can be achieved from 0.35 to 2.7 mm, even with PWV of 1.5 mm. Such sensitivity will allow detailed mapping of the temperature, density, and velocity field at an unprecedented scale. Figure 4 shows plots of ΔT_R for $\delta v = 1 \text{ km s}^{-1}$ for both constant ($\theta_b = 1''$) and for diffraction-limited beams.

In addition to the ALMA requirements for sensitivity, spatial resolution, and spatial dynamic range established for continuum observations, line studies of molecular clouds add velocity resolution (must be easily variable and very fine) and frequency coverage (needed to cover the range of transitions and molecules needed for a full analysis). The baseline ALMA sensitivity for line radiation observed with diffraction-limited resolution and large baselines is marginal. Observing lines at very high spatial and spectral resolution will stretch ALMA to its limit in sensitivity.

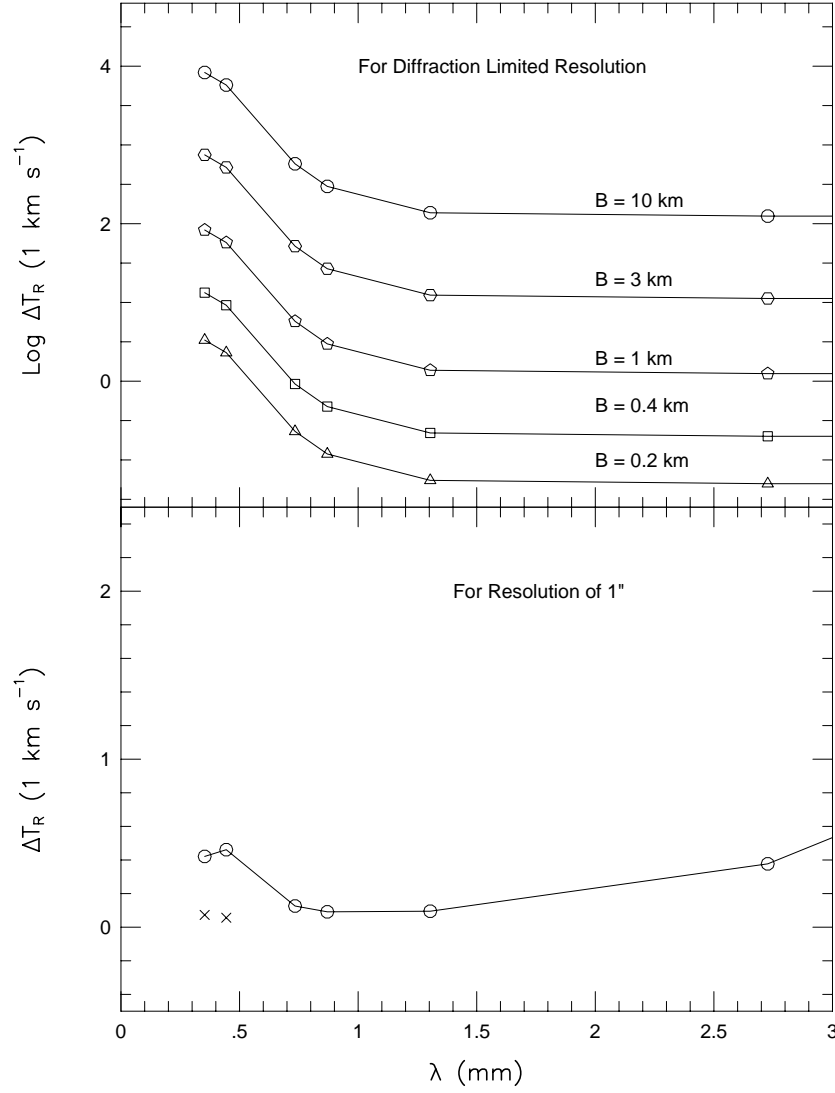


Figure 4. Top Panel: sensitivity to line emission versus wavelength for different maximum baselines; note the logarithmic scale for ΔT_R . Bottom Panel: sensitivity to line emission versus wavelength for constant resolution of $\theta_b = 1''$; note the linear scale for ΔT_R . The crosses at the bottom left correspond to PWV of 0.35 mm; all other points are for 1.5 mm. All values are for a spectral resolution of 1 km s^{-1} .

4. Molecular Line Absorption Against Continuum Sources

This technique, familiar at cm wavelengths, has only recently become possible in regions forming low mass stars (e.g., Choi, Panis, & Evans 1999). The background source is a compact dust continuum source, plausibly a circumstellar disk or perhaps the inner part of the envelope. With current instruments, only a few disks are strong enough to produce absorption lines from molecular gas in front. ALMA will make this a routine probe. Because the disk lies at the center of the infalling envelope, only gas in front of the disk will show absorption, while the rest of the cloud will produce emission. This selection provides a clear-cut way to resolve the infall-outflow ambiguity that plagues studies of cloud collapse. For a beam that includes only an opaque disk, only the front half of the cloud will be seen in absorption. For larger beams, the surrounding cloud will produce emission, resulting in an inverse P-Cygni profile for infall. The sensitivities for line emission are sufficient that most disks can be used in this way.

5. Summary and Requirements

ALMA will provide a tremendous advance in capability for studies of isolated low-mass star formation. The key probes are dust continuum emission and molecular line emission. A new capability, molecular line absorption against circumstellar disks, will become routine, allowing clear-cut resolution of infall-outflow ambiguities.

The requirements on ALMA for dust continuum emission are very low receiver temperatures and wide bandwidths, coverage of a wide range of wavelengths, and very good coverage of the uv plane. The last of these is particularly important, as star formation is intrinsically a multiscale problem, with essential information on scales ranging from a few AU to at least a few times 10^4 AU. For spectral lines, the large bandwidth requirement is replaced by the need for a flexible correlator capable of velocity resolution as good as 0.01 km s^{-1} . The requirement for a wide range of wavelengths is stiffened to essentially complete coverage of the bands that penetrate the atmosphere.

This work has been supported by the State of Texas and NASA grant NAG5-7203. L. Looney and Y. Shirley provided figures.

References

- Adams, F. C., Lada, C. J., & Shu, F. H. 1987, *ApJ*, 312, 788
- André, P., Ward-Thompson, D., & Barsony, M. 1993, *ApJ*, 406, 122
- Bachiller, R. 1996, *ARA&A*, 34, 111
- Butler, B., and Wootten, A. 1999, ALMA Memo. No. 276
- Butner, H. M., Evans, N. J., II, Lester, D. F., Levreault, R. M., & Strom, S. E. 1991, *ApJ*, 376, 636
- Chandler, C. J., & Richer, J. S. 2000, *ApJ*, in press
- Choi, M., Panis, J-F., & Evans, N. J., II 1999, *ApJS*, 122, 519
- Crutcher, R. M., 1999, *ApJ*, 520, 706

- Egan, M. P., Leung, C. M., & Spagna, G. R., Jr. 1988, *Computer Physics Communications*, 48, 271
- Evans, N. J., II 1999, *ARA&A*, 37, 311
- Foster, P. N., & Chevalier, R. A. 1993, *ApJ*, 416, 303
- Goodman, A. A., Benson, P. J., Fuller, G. A., & Myers, P. C. 1993, *ApJ*, 406, 528
- Greaves, J. S., Holland, W. W., Friberg, P., & Dent, W. R. F. 1999, *ApJ*, 512, L139
- Henriksen, R. N., André, P., & Bontemps, S. 1997, *A&A*, 323, 549
- Hogerheijde, M. R., & Sandell, G. 2000, *ApJ*, in press
- Johnstone, D., & Bally, J. 1999, *ApJ*, 510, L49
- Lada, C. J. 1987 in *IAU Symp 115, Star Forming Regions*, ed. M. Peimbert & J. Jugaku (Dordrecht: Reidel), 1
- Looney, L. W., Mundy, L. G., & Welch, W. J. 1997, *ApJ*, 484, L157
- McLaughlin, D. E., & Pudritz, R. E. 1997, *ApJ*, 476, 750
- Motte, F., André, P., & Neri, R. 1998, *A&A*, 336, 150
- Myers, P. C., Evans, N. J., II, & Ohashi, N. 2000, in *Protostars and Planets IV*, ed. V. Mannings, A. Boss, & S. Russell (Tucson: Univ. Arizona), in press
- Rao, R., Crutcher, R. M., Plambeck, R. L., & Wright, M. C. H. 1998, *ApJ*, 502, L75
- Shirley, Y. L., Evans, N. J., II, Rawlings, J. M. C., Gregersen, E. M. 2000, *ApJ*, submitted
- Shu, F. H., Adams, F. C., & Lizano, S. 1987, *ARA&A*, 25, 23
- van der Tak, F. F. S. van Dishoeck, E. F., Evans, N. J., II, Bakker, E., & Blake, G. A. 1999, *ApJ*, 522, 991
- Visser, A. E., Richer, J. S., Chandler, C. J., & Padman, R. 1998, *MNRAS*, 301, 585